

Attractive and repulsive pairing interaction vertices for the two-dimensional Hubbard model

S. R. White, D. J. Scalapino, and R. L. Sugar

Department of Physics, University of California, Santa Barbara, California 93106

N. E. Bickers

Institute for Theoretical Physics, University of California, Santa Barbara, California 93106

R. T. Scalettar

Noyes Laboratory, University of Illinois, Urbana, Illinois 61801

(Received 31 October 1988)

Particle-hole-magnetic and particle-particle-pairing susceptibilities can be expressed in terms of dressed Green's functions and interaction vertices. Using quantum Monte Carlo simulation techniques, the effect of the interaction vertices is examined to determine the sign and relative magnitude of the effective pairing interaction in various channels for the two-dimensional Hubbard model. Near half filling we find that the singlet $d_{x^2-y^2}$ pairing interaction is the most attractive. The extended near-neighbor s interaction is also weakly attractive, while the singlet s_{xy} and d_{xy} and the triplet p_x interactions are repulsive.

The nature of the collective electronic correlations in the two-dimensional (2D) Hubbard model remains an important open question. Of central interest is whether the single-band 2D Hubbard model exhibits superconductivity, and if so, what is the nature of the pairing. It is generally agreed that for a half-filled band, as the temperature is lowered the dominant collective response is associated with the particle-hole staggered spin susceptibility $\chi(\pi, \pi)$. However, the behavior of the pairing correlations in the particle-particle channel of the doped system is less clear. In one view, the spin fluctuations play an analogous role to phonons, with their emission and absorption giving rise to a frequency- and momentum-dependent lifetime, effective mass, wave-function renormalization, and effective particle-particle interaction. In weak coupling, this corresponds to the random-phase approximation (RPA) paramagnon exchange picture,¹ and has been suggested as a mechanism for d -wave pairing in the 2D Hubbard model.² Alternatively, it has been recently suggested³ that a commensurate finite-range spin-density-wave background provides a medium in which dressed quasiparticles suppress the local-spin-density-wave gap, creating a bag; this leads to an attractive singlet s -wave interaction, arising from the "sharing" of the same bag by two holes. In strong coupling, variational projected wave-function calculations⁴ indicate that d -wave pairing is favored. Another view is the resonating-valence-bond theory⁵ in which the spin and charge degrees of freedom of the holes are separated by the strongly correlated background, and the pairing is ultimately mediated by interlayer tunneling.

In the face of this wide range of proposals, it is useful to have some exact results. In principle, quantum Monte Carlo simulations offer this possibility. However, such simulations have so far been carried out only at temperatures which are more characteristic of the magnetic correlation energies than pairing correlation energies.^{6,7} If it were possible to carry out the calculations at temperatures

as low as the assumed T_c , the question of whether the model exhibited superconductivity would be answered by the presence or lack of very strong enhancement in one of the pairing susceptibility channels. At the higher temperatures accessible to current Monte Carlo calculations a different question must be asked: Is the effective pairing interaction attractive? (The energy scales associated with the effective interaction are expected to be much higher than T_c .) Previous calculations⁶ have compared pairing susceptibilities with noninteracting ($U=0$) susceptibilities to determine the nature of the effective pairing interaction, but large single-particle renormalization effects have made the results inconclusive. The slight enhancement or suppression of the pairing susceptibilities due to the effective interaction typically could not be seen because of the much larger suppression due to single-particle effects. In fact, recent studies of electron-phonon models⁸ have shown that an *attractive* interaction can appear *repulsive* at higher temperatures; only at low temperatures does the effect of pairing overcome single-particle effects to show enhancement relative to noninteracting susceptibilities. In this Rapid Communication we suggest an alternative approach which compares pairing susceptibilities with and without the *interaction vertices* included. This comparison allows the determination of signs and relative strengths of the effective pairing interaction in various channels.

The single-band 2D Hubbard model which we have studied is described by the Hamiltonian

$$H = -t \sum_{\langle i,j \rangle, \sigma} \left(c_{i\sigma}^\dagger c_{j\sigma} + c_{j\sigma}^\dagger c_{i\sigma} \right) + U \sum_i n_{i\uparrow} n_{i\downarrow} - \mu \sum_i (n_{i\uparrow} + n_{i\downarrow}). \quad (1)$$

Here the sum on $\langle i, j \rangle$ runs over pairs of near-neighbor sites on a square lattice, t is the hopping integral, U the on-site Coulomb interaction, and μ the chemical potential.

Our basic approach is to use the close relationship of the numerical simulations to standard diagrammatic many-body theory to extract the behavior of the interaction vertices. In the simulation, a Hubbard-Stratonovich transformation is used to replace the two-particle interaction with an effective space-dependent and imaginary time-dependent single-particle field $\{x(l, \tau)\}$. Averaging over all fields $\{x(l, \tau)\}$ with a Monte Carlo sampling procedure restores the interaction. For a given field configuration, the susceptibilities are given in terms of a product of two single-particle Green's functions. Averaging this product over the $\{x(l, \tau)\}$ configurations dresses the Green's functions and generates the interaction vertices shown schematically in Figs. 1(a) and 1(b). Here the solid lines are dressed single-particle Green's functions $G_p(\tau) = -\langle T c_p(\tau) c_p^\dagger(0) \rangle$ and the circles in Figs. 1(a) and 1(b) correspond to particle-hole and particle-particle interaction vertices, respectively. By averaging the single-particle Green's functions over $\{x(l, \tau)\}$ before taking their product, the interaction vertex is removed and one obtains only the first contribution on the right-hand side in Figs. 1(a) and 1(b). This consists of two dressed Green's functions without mutual correlations. We will call this quantity the uncorrelated susceptibility. By comparing the full susceptibility with the uncorrelated susceptibility, we can determine whether the interaction between the dressed quasiparticles is attractive or repulsive.

For example, the staggered magnetic susceptibility takes the form

$$\chi(\pi, \pi) = \frac{1}{N} \int_0^\beta d\tau \langle M(\tau) M(0) \rangle, \quad (2)$$

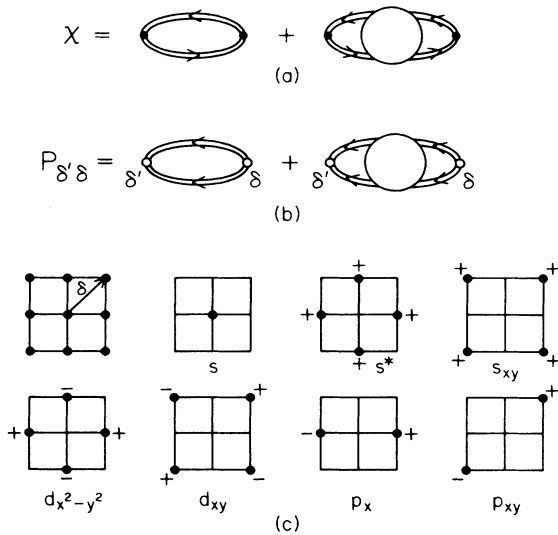


FIG. 1. (a) Diagrammatic representation of the magnetic susceptibility in terms of dressed Green's functions and a particle-hole interaction vertex. (b) The pair-field susceptibility $P_{\delta'\delta}$ expressed in terms of dressed Green's functions and a particle-particle interaction vertex. (c) The internal pair coordinate δ used in defining Δ_δ^\dagger , Eq. (5), ranges over nine positions, including (0,0). The remainder of the figure shows the pair-field modes discussed in the text.

where $M = \sum_l (-1)^l (n_{l\uparrow} - n_{l\downarrow})$ and N is the number of lattice sites. In Fig. 2, $\chi(\pi, \pi)$ is plotted for a 4×4 lattice with $U/t=4$ and two different band fillings. Here one sees the large staggered field response for $\langle n \rangle = 1$ and its suppression when the system is doped slightly away from half filling with $\langle n \rangle = 0.875$. The inset shows the uncorrelated susceptibility

$$\bar{\chi}(\pi, \pi) = -\frac{2}{N} \sum_p \int_0^\beta d\tau G_{p+q}(\tau) G_p(-\tau) \quad (3)$$

with $q = (\pi, \pi)$. Clearly, the particle-hole vertex is attractive, giving rise to a large enhancement of χ over $\bar{\chi}$. The Monte Carlo simulations were carried out using a recently proposed algorithm⁷ which allows the simulation of the 2D Hubbard model at a variety of fillings for inverse temperatures $\beta = t/T$ as large as 8. The algorithm has been tested in a variety of ways, including comparison with exact-diagonalization results on a 2×2 lattice.⁹

In the same way, the particle-particle pairing response can be expressed in terms of dressed Green's functions and an interaction vertex [Fig. 1(b)]. Here we introduce a pair-field susceptibility tensor

$$P_{\delta'\delta} = \frac{1}{N} \int_0^\beta d\tau \langle \Delta_{\delta'}(\tau) \Delta_\delta^\dagger(0) \rangle \quad (4)$$

with

$$\Delta_\delta^\dagger = \sum_l c_{l+\delta\uparrow}^\dagger c_{l\downarrow}^\dagger. \quad (5)$$

The index δ runs over the nine relative lattice spacings shown in Fig. 1(c), and we will discuss the pairing response in terms of the five singlet and two triplet modes (the triplet modes are twofold degenerate) also illustrated in Fig. 1(c). Just as for χ , we use the flexibility of the Monte Carlo simulation to evaluate both the pair-field susceptibility P and the uncorrelated pair-field susceptibility \bar{P} corresponding to the first contribution on the right-

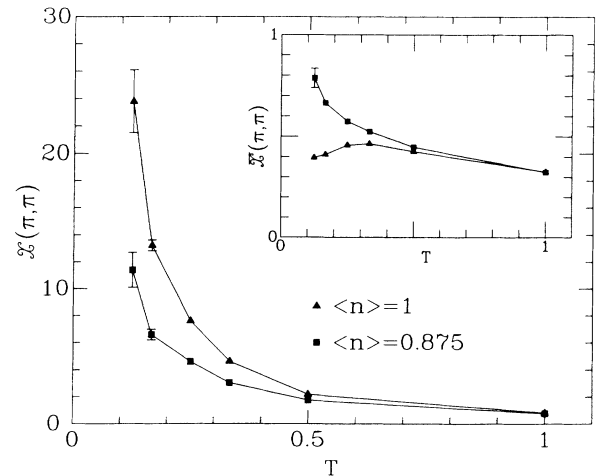


FIG. 2. The staggered susceptibility $\chi(\pi, \pi)$ vs T (in units of t) for a 4×4 lattice with $U/t=4$ and $\langle n \rangle = 1$ and 0.875 . The inset shows the uncorrelated susceptibility $\bar{\chi}$. Where not shown, error bars are smaller than the points.

hand side of Fig. 1(b)

$$\bar{P}_{\delta\delta} = \frac{1}{N} \sum_{ll'} \int_0^\beta d\tau G_{|l'+\delta', l+\delta}(\tau) G_{|l'l}(\tau). \quad (6)$$

P and \bar{P} are plotted in Figs. 3 and 4 for the various pair-field modes shown in Fig. 1(c), with $\langle n \rangle = 1$ and $\langle n \rangle = 0.875$, respectively. Here, as in Fig. 2, $U/t = 4$ and the lattice size is 4×4 .

In Figs. 3 and 4 the solid symbols represent the full susceptibility P while the open symbols represent \bar{P} , the uncorrelated susceptibility. For both fillings the $d_{x^2-y^2}$ mode shows a clear enhancement when the interaction vertex is included. The extended s^* mode also shows a small enhancement while the remaining modes are all suppressed or unchanged by the interaction vertex. The suppression of the on-site s -wave susceptibility by U is clearly evident even at the highest temperatures. However, the suppression of the d_{xy} , s_{xy} , and p_x modes occurs only after the magnetic correlations begin to develop. We believe the dramatic suppression of the d_{xy} and s_{xy} modes for the half-filled case arises from the Pauli principle in the presence of antiferromagnetic correlations; for these modes, Δ^\dagger acts to create a singlet pair at next-nearest-neighbor sites, while the antiferromagnetic correlations imply that spins already exist on these sites, both with spin up or both with spin down. The suppression of \bar{P} (and $\bar{\chi}$) for most of the modes at $\langle n \rangle = 1$ appears to result from a reduction in the density of states, associated with strong

scattering by the antiferromagnetic background. Once the system is doped away from half filling, \bar{P} increases as the temperature is lowered, as one expects for a Fermi liquid.

The size of the $d_{x^2-y^2}$ susceptibility increases as the system is doped from $\langle n \rangle = 1$ to $\langle n \rangle = 0.875$, although the enhancement relative to \bar{P} is greatest at $\langle n \rangle = 1$. As the filling is decreased from $\langle n \rangle = 0.875$ to $\langle n \rangle = 0.75$, results (not shown here) indicate (a) a much smaller enhancement due to the $d_{x^2-y^2}$ vertex [though $P_d (\equiv P_{d_{x^2-y^2}})$ itself remains relatively constant] and (b) a greatly reduced suppression of the d_{xy} mode and somewhat reduced suppression of the s_{xy} mode. This behavior is consistent with the reduction of spin fluctuations as the system moves farther from half filling. To determine the effect of lattice size on the results, the calculations have been repeated on 6×6 and 8×8 lattices for $\beta = 4$. The biggest change with lattice size is a 15–20% increase in the $d_{x^2-y^2}$ susceptibilities both with and without the vertex. The qualitative effect of the vertices is identical to that shown for the 4×4 lattice.

The enhancement of the $d_{x^2-y^2}$ and s^* response and the suppression of the other modes is qualitatively similar to the RPA results obtained in Ref. 2. However, due to the reduction of χ from the RPA result and the suppression of \bar{P} relative to the bare pair-field susceptibility [which would follow from inserting free Green's functions in Eq. (6)], the Monte Carlo result for P_d is much weaker than the simple RPA prediction. Nevertheless, our results would be consistent with a phase diagram for the single-band 2D Hubbard model in which strong antiferromagnetic correlations are suppressed by doping, and d -wave superconducting correlations become important at temperatures significantly lower than those which character-

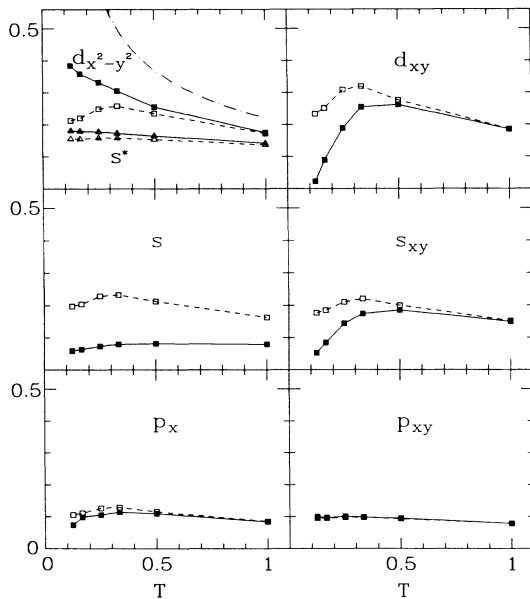


FIG. 3. The pair-field susceptibility P (solid symbols) and the uncorrelated pair-field susceptibility \bar{P} (open symbols) at half filling ($\langle n \rangle = 1$) are plotted vs T for various pair-field modes. Here and in Fig. 4, the noninteracting ($U=0$) $d_{x^2-y^2}$ susceptibility (dot-dashed line) is also shown for comparison. (For the p_{xy} mode, P and \bar{P} are identical to the accuracy of our calculation.)

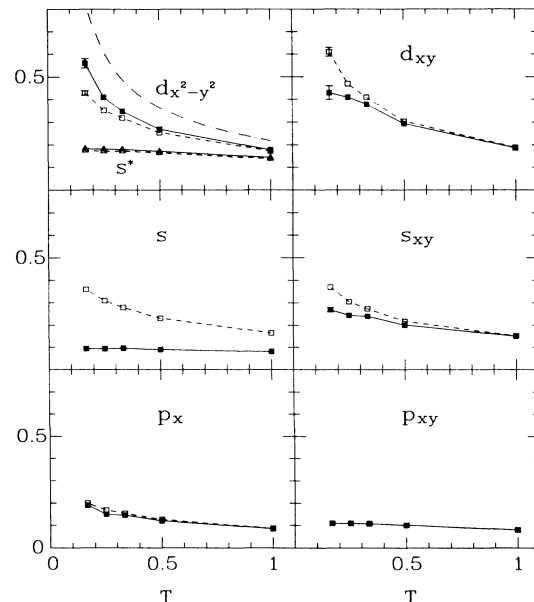


FIG. 4. The pair-field susceptibilities P and \bar{P} vs T for $\langle n \rangle = 0.875$.

ize the half-filled antiferromagnetic correlations. Such a phase diagram would also be consistent with weak-coupling renormalization-group calculations^{10,11} and recent results from self-consistent perturbation theory.¹²

We wish to thank V. Emery and P. Fulde for useful discussions. The numerical work reported in this paper was

done on the Cray XMP at the San Diego Supercomputer Center (SDSC). We wish to thank SDSC for its support. This research was supported in part by the National Science Foundation under Grants No. DMR86-15454, No. DMR86-12860, and No. PHY82-17853; by funds from NASA; and by the U.S. Department of Energy under Grant No. DE-FG03-88ER45197.

¹N. F. Berk and J. R. Schrieffer, Phys. Rev. Lett. **17**, 433 (1966).

²N. E. Bickers, D. J. Scalapino, and R. T. Scalettar, Int. J. Mod. Phys. B **1**, 687 (1987); D. J. Scalapino, in *Proceedings of Symposium S of the Spring Meeting of the Materials Research Society, Anaheim, California, 1987*, edited by D. U. Gubser and M. Schluter, MRS Symposia Proceedings, Vol. EA-11 (Materials Research Society, Pittsburgh, PA, 1987), p. 35.

³J. R. Schrieffer, X. G. Wen, and S. C. Zhang, Phys. Rev. Lett. **60**, 944 (1988).

⁴C. Gros, R. Joynt, and T. M. Rice, Z. Phys. B **68**, 425 (1987).

⁵P. W. Anderson, Science **235**, 1196 (1987); P. W. Anderson, G. Baskaran, Z. Zou, and T. Hsu, Phys. Rev. Lett. **58**, 2790 (1987).

⁶J. E. Hirsch, Phys. Rev. B **31**, 4403 (1985); J. E. Hirsch and H.

Q. Lin, *ibid.* **37**, 5070 (1988).

⁷S. R. White, R. L. Sugar, and R. T. Scalettar, Phys. Rev. B **38**, 11665 (1988).

⁸R. T. Scalettar, D. J. Scalapino, and N. E. Bickers (unpublished).

⁹Our results and those in Ref. 7 show a continuing increase in $P_{d_{x^2-y^2}}$ as the temperature is lowered. This is in contrast to the weak maximum found in $P_{d_{x^2-y^2}}$ by Hirsch and Lin in Ref. 6.

¹⁰I. E. Dzyaloshinskii, Zh. Eksp. Teor. Fiz. **93**, 1487 (1987) [Sov. Phys. JETP (to be published)]; I. E. Dzyaloshinskii and V. M. Yakovenko, *ibid.* **94**, 344 (1988) [*ibid.* (to be published)].

¹¹H. J. Schulz, Europhys. Lett. **4**, 609 (1987).

¹²N. E. Bickers, D. J. Scalapino, and S. R. White (unpublished).